Inferring volumetric changes at a shallow lake from subpixel satellite-derived shorelines

Jesús Palomar-Vázquez [a], Carlos Cabezas-Rabadán [a,b,*], Carmen Castañeda [c], F. Javier Gracia [d], Alfonso Fernández-Sarría [a], Enrique Priego-de-los-Santos [e], Ramón Pons-Crespo [e], Josep E. Pardo-Pascual [a]

[a] Geo-Environmental Cartography and Remote Sensing Group, Department of Cartographic Engineering, Geodesy and Photogrammetry, Universitat Politècnica de València, Camí de Vera s/n, 46022, Valencia, Spain
[b] Univ. Bordeaux, CNRS, Bordeaux INP, EPOC, UMR 5805, F-33600, Pessac, France
[c] Estación Experimental de Aula Dei, EEAD-CSIC, Av. Montañana 1005, 50059, Zaragoza, Spain
[d] Dpto. Ciencias de la Tierra, Facultad de Ciencias del Mar y Ambientales, Universidad de Cádiz, Campus de Puerto Real, 11510, Puerto Real, Cádiz, Spain
[e] Department of Cartographic Engineering, Geodesy and Photogrammetry, Universitat Politècnica de València, Camí de Vera s/n, 46022, Valencia, Spain

Lakes with strong variations in their water coverage may act as indicators of different natural phenomena. Recent techniques for the extraction of Satellite-Derived Shorelines (SDSs) with subpixel accuracy are potentially useful for accurate and continuous monitoring of the limits of water bodies along large periods. This work proposes a method for combining the shoreline position with a digital elevation model to assign elevation values to the points defining the SDSs along the period 1984–2020 in the shallow Gallocanta Lake (NE Iberian Peninsula). The relationship between the water surface and the elevation allows modeling the phenomena of lake changes as well as an estimation of the volume. The obtained data enables analyzing size and elevation changes of the water surface and the volumetric changes of the lake over more than three decades with a sub-weekly frequency (2–5 days). The results constitute a valuable data package for robust analysis of lake trends. In the short term, the methodology provides sufficient precision to capture the changes caused by single meteorological events such as rainfall, even of small magnitude. The method constitutes a novel approach for accurate hydric monitoring of lakes and water bodies, along large territories without requiring continuous *in situ* data acquisition.

1. Introduction

Lakes with strong variations in their water surface offer great importance as indicators of natural phenomena on a local (hydrological response, hydrogeological behavior, human action), regional (aquifer exploitation, general changes in land use) and even global scale (climate change). In recent years there has been an explosion of articles that seek to detect changes in lake water surface (Chen et al., 2018; Palmer et al., 2015; Zhang et al., 2011; Zhou et al., 2019). The monitoring of those changes can provide relevant environmental information. However, the functions and services of the lake as well as its role in hydrological processes will be determined by the water volume, which is not always proportionally related to the water surface area. The analysis of lake volumetric changes enables to estimate the volume of surface inputs that may occur as a result of rainfall events, to define with greater certainty the magnitude of subsurface or groundwater input, and to identify losses due to evapotranspiration, infiltration, or direct abstractions. The simplest method to characterize the water changes of a water body is to have a continuous record of the water level utilizing a ruler driven into the lakebed. This information, which is not always available, can be

* Corresponding author. Geo-Environmental Cartography and Remote Sensing Group, Department of Cartographic Engineering, Geodesy and Photogrammetry, Universitat Politècnica de València, Camí de Vera s/n, 46022 Valencia, Spain.
E-mail address: carcara4@upv.es (C. Cabezas-Rabadán).

ineffective in intermittent shallow lakes in which water surface can occur in separated ponds during low water episodes. Moreover, in order to obtain robust measurements, the altitudinal position of the ruler must remain completely stable over time, and this is often not the case for shallow saline lakes or lakes with strong water level fluctuations (Castañeda & Herrero, 2005).

Remote sensing techniques have been widely used to study lake and reservoir water changes (Crétaux et al., 2011). They allow the acquisition of data covering large territories without the necessity of *in situ* human intervention, offering high potential for systematic monitoring at continental-scale, even in remote areas. Water elevation may be defined by altimetry missions based on radar as TOPEX/Poseidon (Birkett, 1995), Envisat (Frappart et al., 2006), Cryosat-2 (Villadsen et al., 2015), SARAL (Schwatke et al., 2015), or LIDAR as ICESat (Zhang et al., 2011) and ICESat-2 (Cooley et al., 2021; Zhang et al., 2019). Water coverages are delimited also from radar using high-spatial-resolution sensors (e.g. Gstaiger et al., 2012) while products derived from freely available missions are constricted due to their coarse spatial resolution (e.g. Xing et al., 2018; Gulácsi & Kovács, 2020). Optical images have been used to define water coverage based on reflectance differences in their single bands or a combination of them by creating indices (Huang, Nguyen, Zhang, Cao, & Wagner, 2017). Global databases of water bodies have been generated defining the current state and their changes over time (Busker et al., 2019; Pekel et al., 2016; Schwatke et al., 2015). Despite their great contribution for studying the coverage of large water bodies such as those experiencing variations of several meters throughout the year, the accuracy of these techniques is reduced for smaller lakes (Crétaux et al., 2011). The analysis of the volume has been approached from bathymetry or the elevation of the water body combined with DEMs. Thus, under the assumption that the water surface is flat over a certain area, Penton and Overton (2007) suggested approaching the volume definition by the integration of the water extent with elevation data. Thus, the integration of different data sources has led to the estimation of the volumetric changes of the water bodies (e.g. Zheng et al., 2016; Zhu et al., 2014). Most of these works focus on lakes that undergo important altitudinal changes (meters), something that does not occur in shallow lakes. Due to the limitations imposed by pixel size and altimetric accuracy, the previous techniques may become useless for monitoring small/shallow water bodies. In those spaces, the smallest volumetric changes can have significant ecological consequences, especially in the coastal fringe, where ecological gradients and biodiversity achieve their greatest values (Castañeda et al., 2020).

An alternative method for estimating the stored water comes from determining the three-dimensional position of the shore. This procedure requires both a DEM that includes the surface of the bottom of the lake and numerous and highly-accurate records of the shoreline position along time. The recent availability of algorithms for extracting Satellite-Derived Shorelines (SDSs) with subpixel accuracy (e.g. Sánchez-García et al., 2020) and tools as SHOREX (Cabezas-Rabadán et al., 2021) opens up the possibility of efficiently managing a large volume of data over decades.

The aim of this research is the continuous estimation of lake volumetric changes using SDSs extracted from Landsat and Sentinel-2 imagery and a DEM of the bottom of the lake. The study considers changes along 35 years in the Gallocanta Lake (NE Spain), a shallow saline lake that undergoes strong variations in its water surface extent.

2. Study area

2.1. Regional setting

Gallocanta Lake is located in NE Iberian Peninsula (Fig. 1), within the Iberian Range, a NW-SE oriented intraplate mountain system with moderate relief generated during the Alpine orogenic cycle. The range includes several inner basins, most of them of tectonic origin. However, following Gracia et al. (2002) the lacustrine basin hosting Gallocanta
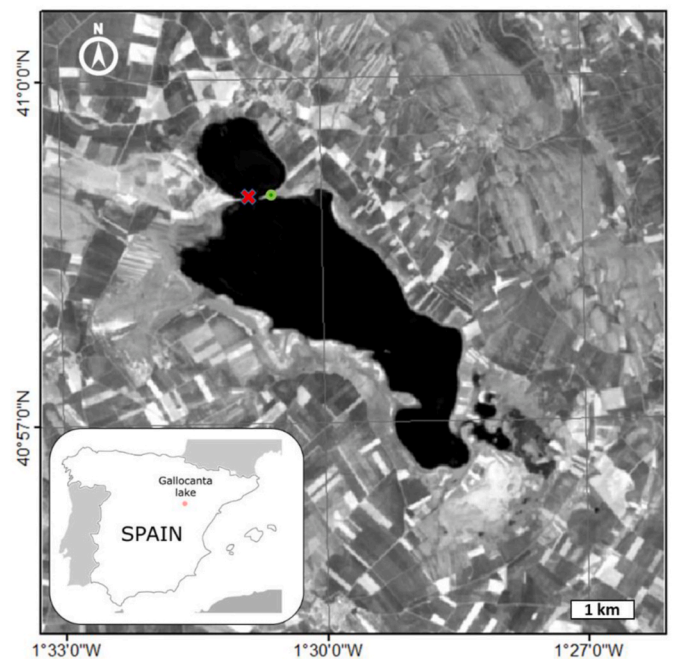

Fig. 1. Location of the Gallocanta Lake (NE Spain), the limnigraph (green dot) and the ruler (red cross) currently employed to derive the water level.

Lake has a karstic origin, related to the transformation of a former karst polje on carbonates into an endorheic closed basin during the Late Pleistocene.

The lacustrine basin, oriented parallel to the prevailing winds, is surrounded by low ranges on Palaeozoic quartzites (NE), Mesozoic carbonates (SW), and Neogene conglomerates (NW and SE). Its substratum is mainly constituted by Triassic evaporites and clays, which have made the lake to acquire a highly saline nature. At present, it is a hypersaline lake of the Na–Mg–Cl-(SO$_4$) type (Comín et al., 1990), where strong evapotranspiration and intense unidirectional winds favor its desiccation and the precipitation of salts often covering the bottom of the lake. The climate is semiarid with a mean annual rainfall of 488 mm over the last 70 years, irregularly distributed. García-Vera and Martínez-Cob (2004) characterized the meteorological data in the lake for the period 2005–2014 from the automatic weather station located next to the limnigraph (Fig. 1). The mean annual temperature is 11.2 °C. The annual hydric deficit is 605 mm and the reference evapotranspiration (ET$_0$) higher than 1000 mm year^{-1} at the lake borders. The frequent NW winter winds reach speeds of >80 km h^{-1} (Martínez-Cob et al., 2010, p. 200). In recent decades, a general trend towards decreased flooding has been observed associated with a highly fluctuating climate. As a consequence, from a maximum lake water level of almost 3 m registered in 1974 the lake may now desiccate completely in years of low rainfall (Castañeda et al., 2015).

The present lake bottom is completely flat, while the shores are formed by gentle beaches with very fine sands. The NE margin of the basin is represented by a set of alluvial fans and pediments with a mean slope of 4%, whose distal areas are perched about 6 m over the present lake bottom. Streams in this margin are intermittent, inset on the fans, forming flat-bottomed valleys which historically gave this margin an irregular, highly indented outline. In contrast, the SW shore is formed by a very gentle surface (mean slope <1%) on a large fan whose lowest area connects with the present lake shore.

The lake has notable environmental importance and hosts several protection figures (National Hunting Refuge, Wildlife Refuge of International Interest, Zone of Special Protection by the European Birds Directive, etc.). In 2006 it was declared Nature Reserve, as it constitutes an extraordinary important station for European migratory birds (Castañeda et al., 2020).

3. Available data

As source data has been considered (a) all the Landsat and Sentinel-2 satellite imagery acquired between June 1984 and June 2020 to define the shoreline position, (b) digital elevation models of the study area, and (c) records of the water level.

a) Satellite imagery:

The images acquired by the satellites Sentinel-2 (sensor MSI) and Landsat 5 (TM), 7 (EMT+), and 8 (OLI), of equivalent quality (Fig. 2) are available free of charge from the Copernicus Open Access Hub and the Earth Explorer of the U.S. Geological Survey (USGS). The whole study period is covered by Landsat missions: Landsat 5 (from 1984 to 2011) is followed by Landsat 7 (from 1999), and Landsat 8 (from 2013). Sentinel-2 mission became operational in 2015 with the satellite 2A followed by its twin 2B in 2017. While Landsat missions offer a revisit time of 16 days, the Sentinel-2 constellation provides a revisit of 5 days. The revisit has been reduced along the study period because of the overlap of the different missions, reaching at the end of the period a time about 2.9 days when the satellites are combined (Li & Roy, 2017). It should be noted that from May 31, 2003 onwards, Landsat 7 images present data gaps associated with the Scan Line Corrector (SLC) failure. For this reason, the period between November 2011 (when the acquisition of Landsat 5 images stopped) and April 2013 (Landsat 8 images became available) showed the least frequent characterization of the shore position. The images of all these satellites offer the bands RGB, NIR, SWIR1, and SWIR2, employed within the extraction process. They offer middle spatial resolution (10–30 m) and radiometric characteristics that, as described in Pardo-Pascual et al. (2018) and Sánchez-García et al. (2020), allow the extraction of comparable SDSs.

b) Digital Elevation Model

The work relies on the elevation data for the entire area that is flooded at some point during the study period.

A DEM from LiDAR data by the National Geographic Institute of Spain (IGN, https://pnoa.ign.es/el-proyecto-pnoa-lidar) was used for this purpose. The original raw data were acquired during October 2010, at a time when the lake showed a low water level, but it was not desiccated. Regarding the accuracy of the LIDAR records, the point cloud showed an average density of 0.5 points/m^2 and the altimetric accuracy of each point was better than 20 cm (RMSE). Since the center of the lakebed was covered by water, in certain parts the altimetric information was missing. However, as the lakebed bottom is extremely flat, the data recorded offered sufficient spatial resolution to interpolate the areas without signal.

c) Lake water level

The water level in the Gallocanta Lake has been obtained along the years by the Ebro River-Basin Authority from field data (CHE, 2003), using limnigraph measurements adjusted according to rulers installed into the deepest point of the lakebed (see Fig. 1). The harsh environmental conditions (e.g. episodes of significant wind, waves, high salinity, and intermittent desiccation cycles) made it difficult to maintain the infrastructure calibrated, hindering the collection of field measurements from the rulers and eventually making it necessary their successive replacement. This limitation of the data from rulers has been described in similar environments (Castañeda & Herrero, 2005) and resulted in data gaps and the disconnection between series of water level data acquired along time, therefore limiting their use for the calibration or validation of hydrological data.

4. Methods

The volume deduction is based on the obtention of Satellite-Derived Shorelines and their combination with the DEM (Fig. 3).

4.1. Satellite-Derived Shorelines

The downloading of the satellite imagery, pre-processing, and extraction of SDSs were carried out using the system SHOREX (Cabezas-Rabadán et al., 2021). After the downloading, manual cloud-checking allowed to discard those images with clouds covering the shore of the lake. Subsequently, the SDSs were automatically defined from 1043 images as the water/land intersection at the acquisition time of each image. Firstly, the position of the shore was approximately defined at pixel level by a mask created according to the AWEINSH index (Feyisa et al., 2014) setting a constant threshold value of 0. Taking the approximate line at pixel level as reference the shoreline was extracted applying the subpixel algorithm proposed by Pardo-Pascual et al. (2012). This procedure operates over the Short-Wave Infrared bands (SWIR1) using a third-degree polynomial and 3x3 analysis kernel. The accuracy of the resulting SDSs has been evaluated on multiple occasions in different environments, showing accuracies (expressed as RMSE) between 3.5 and 4 m (for S2 and L8 images respectively) on the low-energy microtidal sandy beach of Cala Millor, Mallorca (Sanchez-García et al., 2020), 4.55 m on the microtidal and highly-energetic Reñaca Beach, Chile (Sanchez-García et al., 2019), and between 4.6 and 5.7 m (S2 and L8, respectively) on the exposed mesotidal Faro Beach, Portugal (Cabezas-Rabadán et al., 2020). Previously to this study, a specific validation test was made in the Gallocanta Lake (Palomar-Vázquez et al., 2019) by comparing the shoreline position defined in-situ using DGNSS (Fig. 4) with the SDS extracted from an S2 image acquired on the same day. The resulting accuracy of 4.15 m RMSE is very similar to the one recorded in the rest of the assessments on marine beaches.
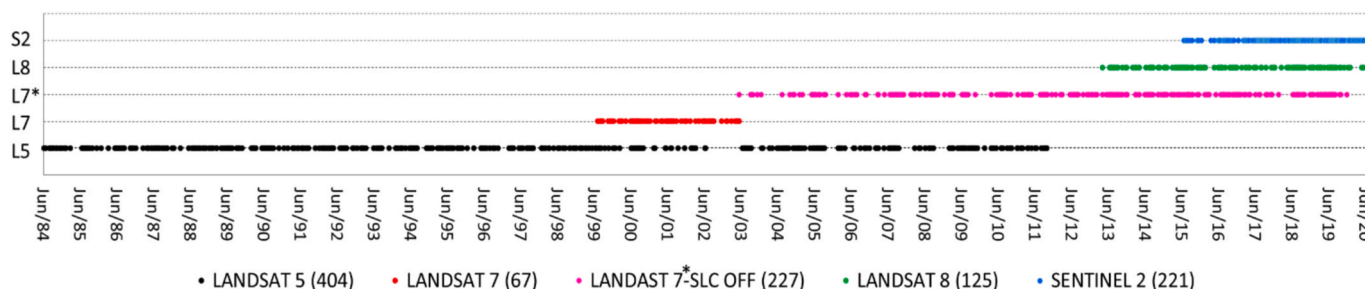

Fig. 2. Available images from the different sensors. Landsat 7 shows data gaps after May 31, 2003 due to the SLC failure, but when available they are still useful and maintain the same radiometric and geometric corrections.
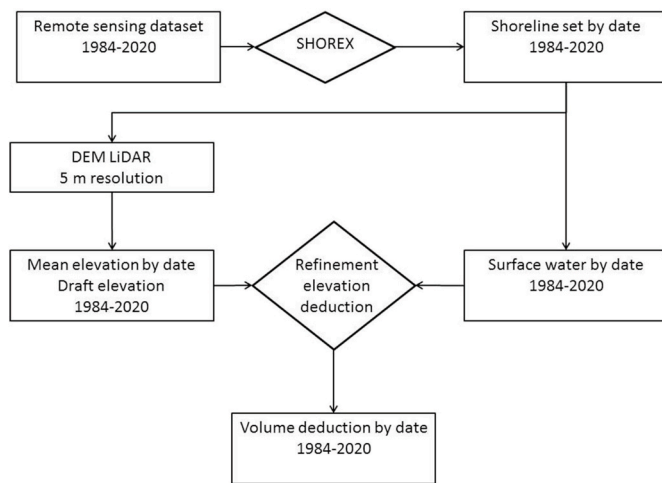
Fig. 3. Workflow of the methodology for volume deduction.

4.2. Water surface

The large set of SDSs enabled to define the lake surface and its size changes throughout the study period. A polygon delimiting the water at the pixel level was defined, and its contour was adjusted according to the position of the points that define the shoreline at the subpixel level. Regarding the L7 images acquired with the SLC-off, the data gaps in the mask defined by the AWEINSH were filled using morphological filters to carry out the definition of a continuous water surface.

4.3. Mean elevation of the water level

The estimation of mean elevation relies on the assumption that the water surface is flat over a certain area (Penton & Overton, 2007). Taking this into account, for each date the three-dimensional position of the shore was determined by assigning the elevation data of the DEM to the shoreline points and calculating the mean elevation. In this operation, only the western half of the lake was considered since it has gentler

Fig. 4. In-situ definition of the shoreline position in the Gallocanta Lake using a DGNSS system (May 14th, 2019). The flat morphology of the shore creates a smooth gradation of highly-saturated soil along the land/water interface causing difficulty in defining the real shoreline.

slopes and, therefore, the positioning errors of the SDSs will have a lower impact on the elevation values.

This solution made it possible to obtain elevation data individually for each date strictly based on the shoreline position and the DEM. Nevertheless, in order to minimize the potential errors of those data sources, a refinement of the elevation deduction was proposed. It was based on modelling the relationship between the water surface and the elevation obtained from the whole dataset, assuming that larger lake surfaces must be associated with higher water levels. The pairs of surface and elevation values recorded over time were numerically related employing a third-degree polynomial function. This equation represents the phenomenon of elevation increase associated with larger surface areas as it is experienced in Gallocanta Lake. The substitution of the values of the lake surface at different dates in the refined model enables to obtain the corresponding elevation.

4.4. Volume estimation

In order to determine the volumetric changes along time, the elevation and the surface area of each date were compared with those obtained for the first date of the study period. Subsequently, multiplying the surface and elevation differences allowed the obtention of the relative volumetric changes. The date with the largest negative volumetric change was identified and assimilated to the complete desiccation of the lake, therefore assigning a value of zero volume. The whole series was recalculated by adding the relative volumetric change value of that reference date, converting all the volumetric values into absolute volumes.

5. Results

The position of the shoreline was defined on 1043 instants, which together with their associated elevation allowed to define the water surface size, the mean elevation and its changes through time, and the relative changes of the water volume.

5.1. Water surface

Along the period 1984–2020, the area of Gallocanta Lake experienced variations along time, fluctuating between the complete drying of the lake and maximums over 12 km^2 (Fig. 5). Notwithstanding these important variations, the lake area varied around an average value of 6–7 km^2 (mean of 6.07 and median of 7.07 km^2). The lake showed a large surface area continuously from 1987 to 1993, and the maximum of 12.36 km^2 registered on January 31, 1992. Afterward, the lake experienced several periods of complete desiccation, alternating with annual and bi-annual periods over 8 km^2 (e.g. 2003–2005, 2013–2015), and reaching an area of 11 km^2 at the end of the spring of 2020 for the first time since the early 1990s.

5.2. Water level elevation

When the values of the water surface of the lake are related to the mean elevation of the shoreline, a direct but non-linear relationship appears (Fig. 6). Although a clear trend can be observed, the pairs of data recorded at different dates show some dispersion. Taking this into account, and in order to minimize the effect of this punctual dispersion in the elevation series, the elevation is not directly defined using the values of DEM coincident with the shoreline location. In turn, it is deduced from the lake surface of each date according with the polynomial function fitted to the whole data set. The fit between both variables is very high (r^2 about 0.98), showing a low weight of the errors related to the inaccuracies associated with the DEM and the positioning of the shorelines. Furthermore, the model obtained shows an obvious characteristic of the lake, which is that in its central part it is extremely flat and has a slightly steeper slope in its external part.
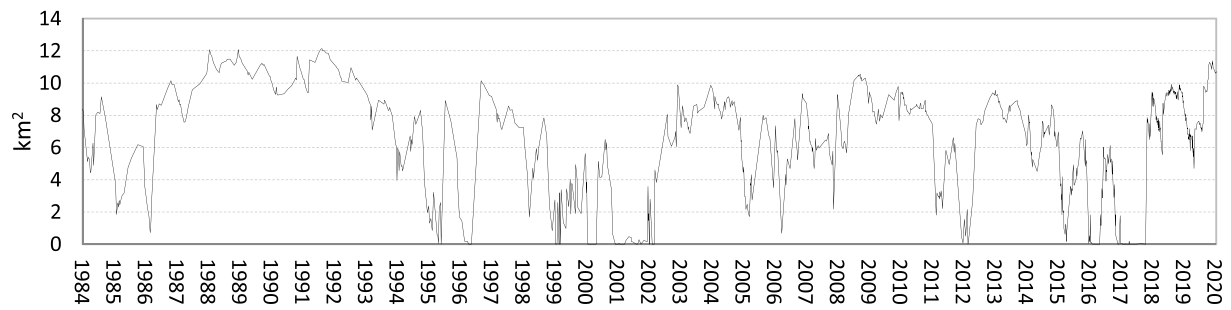
Fig. 5. Water surface fluctuations (1984–2020) extracted from satellite data.

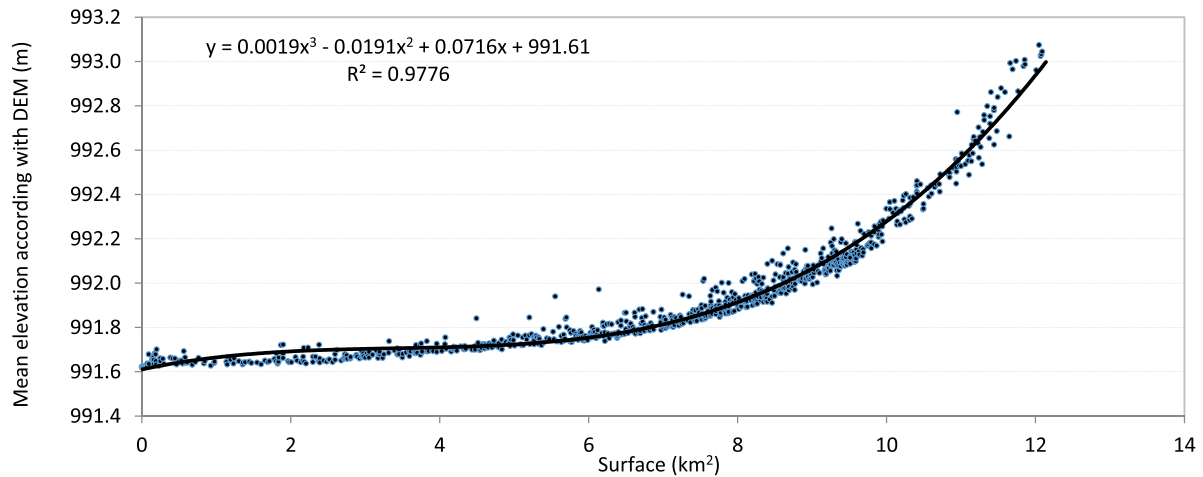$$y = 0.0019x^3 - 0.0191x^2 + 0.0716x + 991.61$$
$$R^2 = 0.9776$$

Fig. 6. Numerical relationship between the lake water surface and its mean elevation according to the DEM (blue dots), and the numerical model relating both variables (black line).
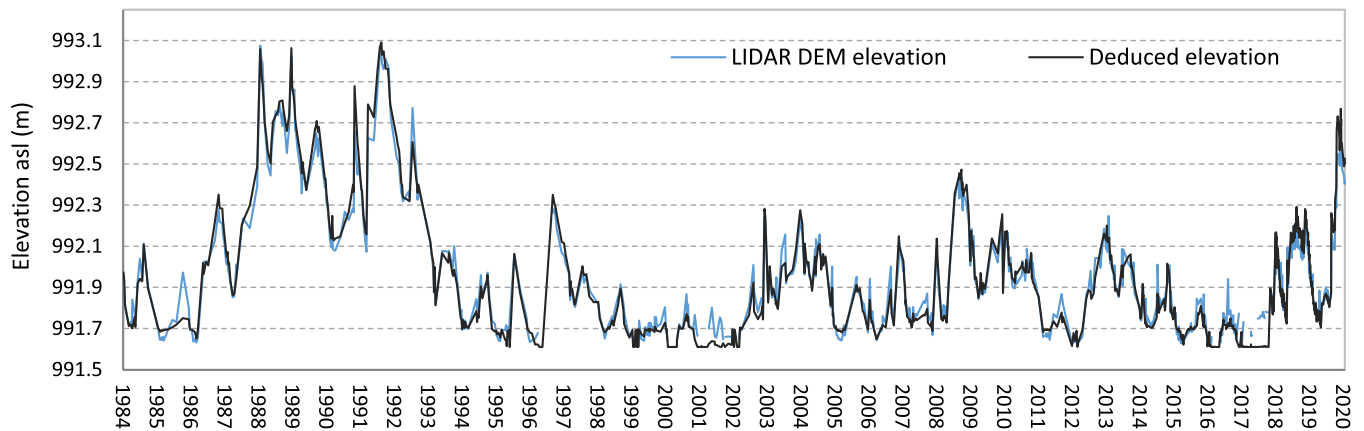

Fig. 7. Elevation above sea level of the water surface deduced both from the DEM (blue line) and from the numerical function (black line).

When comparing the surface elevation obtained directly from the DEM data associated with the shoreline position versus the elevation deduced from the numerical function (Fig. 7), it is possible to observe how they represent similar trend changes over time.

5.3. Volumetric changes

The lake experienced great volumetric changes along the study period, from several periods of complete desiccation to over 17 hm^3 during the late 1980s and early 1990s. From 1988 to 1993 the lake
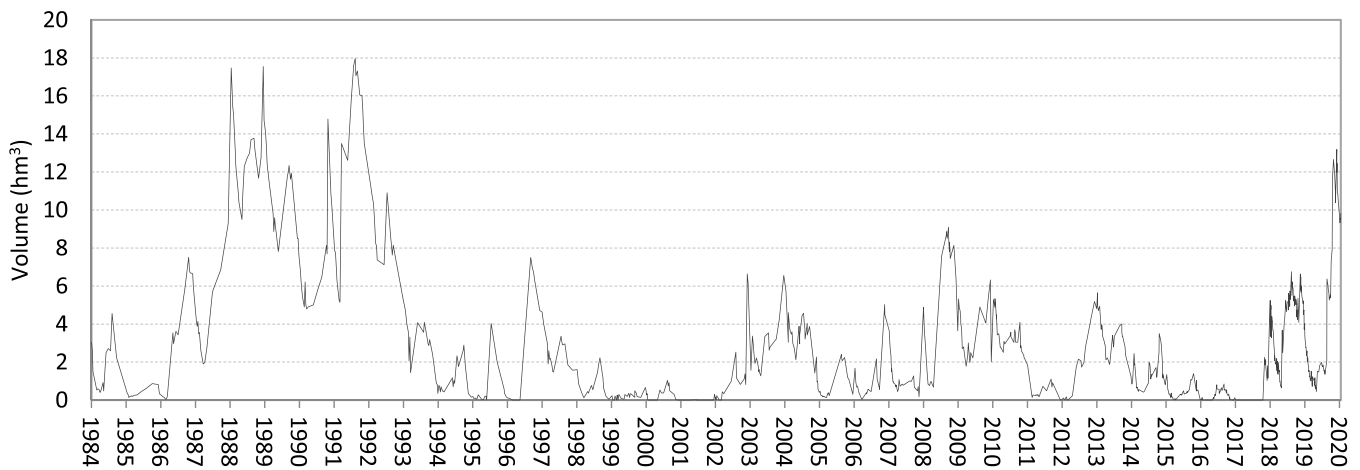
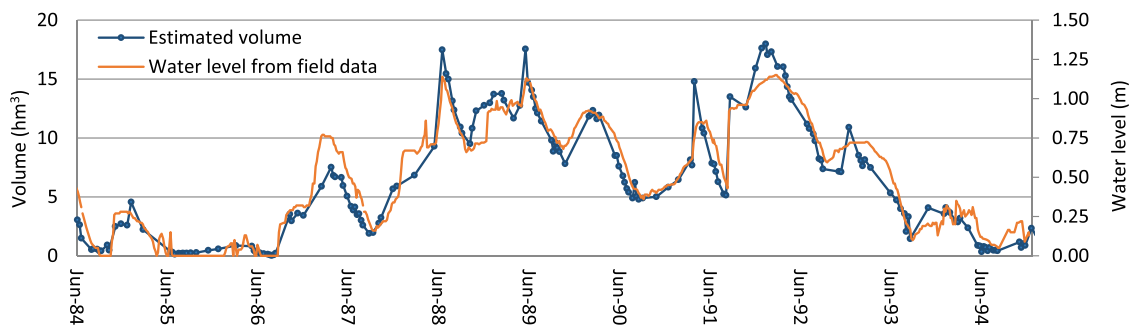**Fig. 8.** Evolution of the estimated water volume (1984–2020).

Fig. 9. Evolution of estimated water volume (in blue colour, with the employed satellite images as points) and water level (in orange) according to field (limnigraph and rulers) registers from June 1984 to December 1994.

followed a filling period, showing volumes above 6 hm^3 and peaking close to 18 hm^3 during February 1992. After that time, the volume stayed low, and only at specific times the 6 hm^3 were exceeded. A peak of 13 hm^3 reached during spring 2020, almost at the end of the series of records, stands out.

6. Discussion

Recent techniques have been developed to achieve an efficient extraction of the coastal shoreline position associated with large volumes of dates from mid-resolution satellite imagery. The present paper proposes to apply the system SHOREX for shoreline extraction to lake monitoring, offering the continuous acquisition of detailed information on changes in the water presence without the need for *in situ* data. Thus, the surface covered by the Gallocanta Lake, its elevation, and its volume have been estimated over 36 years.

6.1. Water changes in Gallocanta Lake

The definition of the shoreline position at subpixel level has been used to accurately define the shape and perimeter of Gallocanta Lake at 1043 instants over the period 1984–2020 (Fig. 5). The surface has experienced important changes along time, alternating periods of complete desiccation and others above 12 km^2. This surface is below the more than 14 km^2 recorded during the especially wet decade of the 1970s (García-Vera et al., 2009, pp. 77–101; San Román et al., 2007), and far from the 20 km^2 estimated in the 1920s by Hernández-Pacheco and Aranegui (Galván, 2011).

The high accuracy of the shoreline dataset in combination with a DEM allows to define the elevation of the water surface and their

changes (Fig. 6). Throughout the study period, the elevation values vary in a range of about 1.5 m. When compared with the surface values, it can be observed that both variables do not strictly follow the same pattern of changes. This is partly since, after the 1990s, the lake has low levels and the shoreline is located in areas of a very gentle slope, which translates into almost negligible variations in elevation.

The estimated elevation could be compared with the field water level records (using limnigraph and rulers) in the Gallocanta Lake. The pattern of change experienced by the estimated water volume seems consistent with the field measurements (Fig. 9). Relatively small lack of coincidence between the two data sources may be appreciated along the series, partly as the estimation of the volume is limited by the availability of satellite images.

Nevertheless, the field measurements defining the water level suffer also limitations and should be considered with caution. On the one hand, some locations of the successive rulers employed might have been disconnected from the water ponds spread on the lakebed when water levels were very low. On the other hand, the alternating drought and flooding periods of the lake underwent significant changes in the consistency and density of the lakebed salt-rich sediments, which probably lead to changes in volume. Thus, due to the high difficulty of finding representative results from combining the ruler-based water level measurements and the satellite imagery, the formers have not been considered to calibrate the estimates by remote sensing data.

The estimation of lake water volume and its changes from the large dataset presented in this work enables to identify both short- and medium-term changes in lake water. On an annual scale, it is possible to observe cyclical oscillations, although significant differences appear among years (Fig. 10). Seasonal variations are also observable. Water volume depletions appear during the summer seasons, while autumn
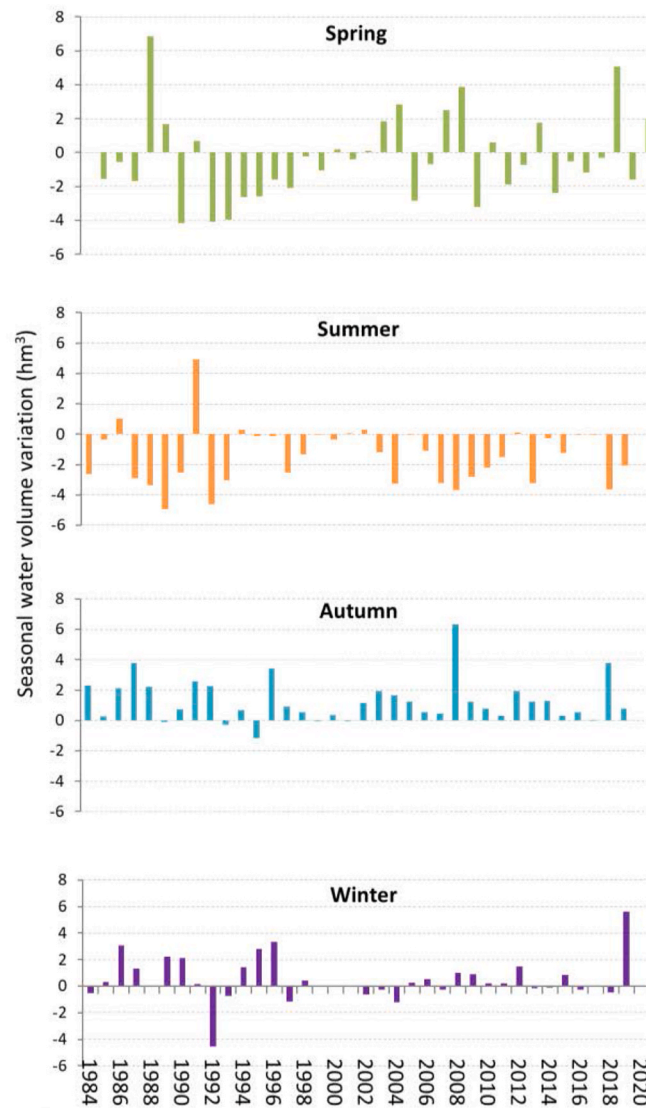
Fig. 10. Seasonal water volume variation (hm^3) in the Gallocanta Lake, from 1984 to 2020. The four seasons have been defined considering as starting day the 21st of December (winter), March (spring), June (summer), and September (autumn) respectively.
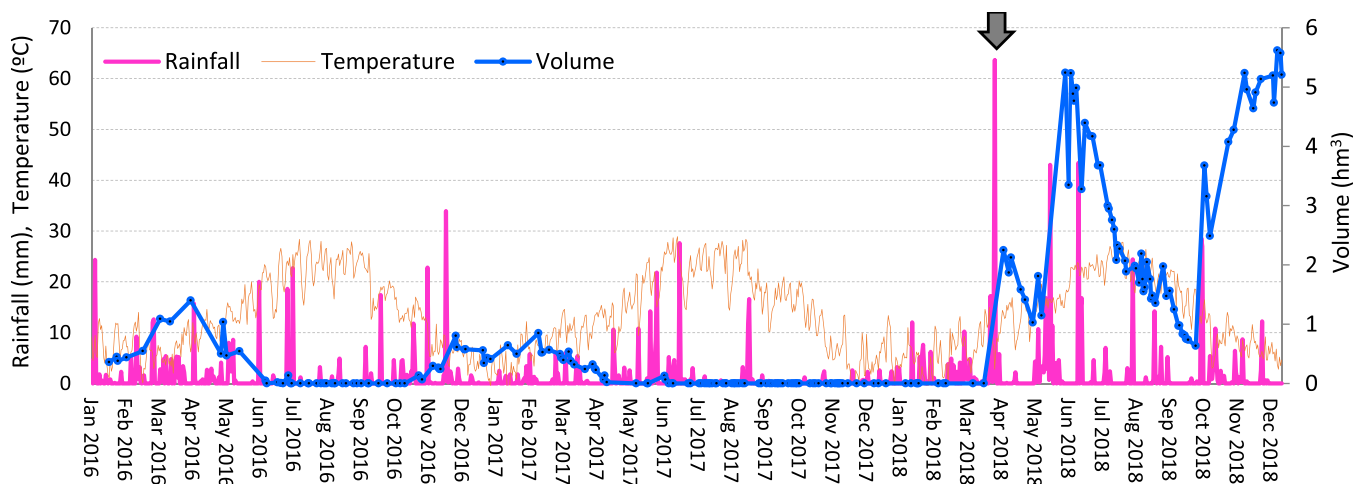
Fig. 11. Estimated water volume through the period January 2016–December 2018 together with the daily rainfall and average temperature data obtained from Daroca weather station (Spanish Meteorological Agency, AEMET) as representative of the weather conditions in Gallocanta Lake (Luna et al., 2014, p. 164). The arrow highlights the rainfall event in early April 2018 associated with an outstanding lake volume increase also illustrated in Fig. 12.
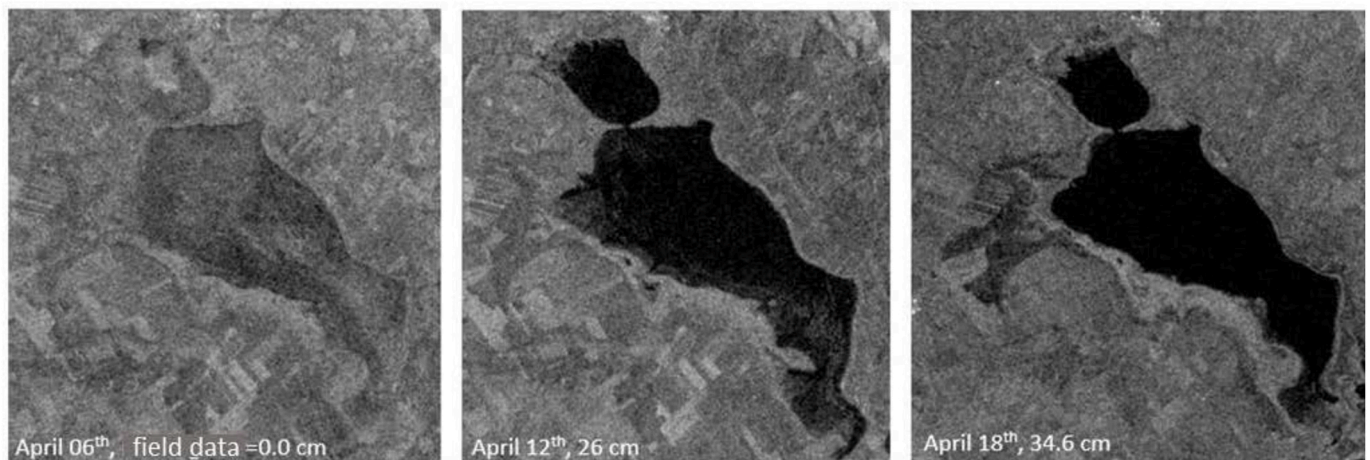
Fig. 12. Sentinel-1 VV polarization images from April 06th, 12th, and 18th 2018 suggest a filling process in the Gallocanta Lake associated with the transition between dry (April 6th) and flooding conditions (April 12th-18th), after the 95 mm of rainfall registered between April 7th and 11th in Daroca weather station (see Fig. 11).

and winter show volume gains that are remarkably higher during autumn. This is greatly linked to the differences in precipitation and temperature recorded throughout the year in the Gallocanta Lake area. Seasonal volumes partly contrast with rainfall registers, but it is important to highlight that within seasons with a prevalence of losses the lake still may flood or increase its volume associated with rainfall episodes and hydrogeological inputs. Nevertheless, the highest temperature and sun irradiation experienced during late spring and summer accelerate the evaporation and reduce the water volume of the lake. Although changes in precipitation and evaporation throughout the year are important factors controlling the water volume (Fig. 8), the results of the present work corroborate that it does not strictly follow a seasonal pattern. Water surface variations in the lake reflect not only the prevailing climatic conditions but also those of previous periods (Comín et al., 1990). Thus, after several consecutive climatically wet years, the lake tends to show and maintain a larger amount of water, as it was in the early 1990s. On the contrary, lower lake water volumes can be associated with recurrent episodes of desiccation during the summer. This is the case of 2001, showing desiccation throughout much of the year, being one of the driest years on record and associated with a dry period (Luna et al., 2014, p. 164).

The detailed characterization of volume changes achieved in the last four years shows important coincidences with the meteorological conditions in the surroundings of the lake (Fig. 11). Precipitation recorded during the day or days before the acquisition of the satellite image has resulted in increases in water volume. It is also interesting to note the rapid reduction in lake dimensions when its volume is low and the temperatures are high. This is especially noticeable in summer when water surfaces of several kilometers disappear in a matter of days associated with high temperatures.

In 2018, the fast change between the dry state of the lake (April 6th, field data show 0.0 cm) and its filling after the rains (April 12–18th, 26 and 34.6 cm according with field data) has been recorded by the Sentinel −1 C-band radar images (Fig. 12). Even though their lower resolution and the complexity of the backscattering response impedes a highly accurate delimitation of the lakebed and the water surface extent, the visual inspection of the C-band images evidence the increase of the water level and its growth in parallel with rainfall episodes (Fig. 11).

6.2. A new method for volume estimation based on SDSs

Water surface monitoring is based on the high spatial accuracy of the shorelines extracted by SHOREX, which have been recently applied to analyze geomorphological changes in marine coastal environments (e.g.

Cabezas-Rabadán et al., 2019; and 2021), but never on inland water bodies. This methodology based on extracting the shoreline position per date contrasts with the remote sensing techniques mostly used to monitor inland water bodies, lakes, and reservoirs. From optical satellite imagery, numerous works and databases have already delimited the water bodies over time covering large territories, even on a global scale (e.g. Busker et al., 2019; Pekel et al., 2016). However, most of these works offer pixel-level accuracy and, therefore, little capacity to identify water surface changes of small dimensions. The methodology based on subpixel extraction of the shoreline offers higher accuracy in delimiting the water bodies and in detecting changes, even those of small magnitude. The traditional pixel-scale detection of the shoreline relies on the thresholding of the image after the calculation of the water index. This constitutes only the first phase of the sub-pixel solution employed in this work (SHOREX), after which a 3x3 pixel neighbourhood (corresponding to 60 or 90 m for S2 and Landsat imagery respectively) is scanned around the shoreline defined at the pixel level to find the position of the shoreline more accurately, reaching an error about 4–5 m RMSE. This is a particularly significant advance in small lakes with abrupt changes in their flooded surface as the Gallocanta Lake. In addition, the subpixel SDS provides information not only on the flooded area but also on its detailed shape. This can offer information about lake morphometry and changes of ecological importance because the rapid shoreline changes that occur in shallow and fluctuating lakes determine the habitat distribution and the preservation of protected species (Timms, 1992, p. 180).

The methodology proposed in this work is supported by the high spatial resolution of the shorelines extracted by SHOREX, with values close to 3–5 m RMSE (Sánchez-García et al., 2020; Palomar-Vázquez et al., 2019). Although inland water bodies lack the dynamism and swash processes that may pose a challenge for defining the shoreline position in marine coastal environments (Cabezas-Rabadán et al., 2020), a shallow lake like Gallocanta brings other difficulties for the definition of the land-water interface. The occurrence of sheets of water only a few centimeters thick covering significant areas together with zones where the soil is saturated in water (see Fig. 4) sometimes makes it difficult to delimit the water surface. The challenge of defining the approximate shoreline position, a step required by SHOREX prior to starting the extraction process, has been solved by adopting the AWEINSH index (Feyisa et al., 2014) after offering satisfactory results in previous tests in Gallocanta Lake (Palomar-Vázquez et al., 2019). This has allowed achieving the automation of this part of the process, increasing the objectivity of the results and facilitating the obtention of a large SDS dataset.

The revisiting of satellite images from the Landsat and Sentinel-2 series enables to have a large dataset of the lagoon morphology covering more than 3 decades. The distribution of images is uneven over time, with higher density in the final part of the series. At present, the combination of satellites L8, S2A, and S2B offers a revisit time of about 2.3 days (Li & Chen, 2020) enabling the quantification of changes in the water sheet with sub-weekly frequency. This large availability of data is being increased even more with the recent availability of Landsat-9 images.

The solutions proposed in the literature to define the elevation in lakes either are based on payment platforms (e.g. TerraSAR-X) and/or do not offer sufficient spatial or altimetric resolution to be useful in shallow water bodies. Thus, when a DEM is available (using bathymetric techniques or aerial sources in the case of lakes experiencing seasonal drying processes), the methodology presented here seems to be a very interesting alternative for an accurate definition of elevation, especially in water bodies with reduced slopes. The accuracy of the subpixel shorelines is key in this methodology in order to correctly define the three-dimensional position of the shore and, consequently, its elevation. The proposed refined elevation model is defined by the numerical function that relates a large dataset of surface and elevation data intending to minimize the influence of existing errors in the definition of the shorelines and in the DEM itself. The raw data of the model have been obtained from LIDAR, with an estimated altimetric accuracy better than 0.2 m RMSE. This level of error is significant considering that Gallocanta Lake is a shallow lake with very gentle slopes. In fact, when comparing the elevation values obtained directly from the DEM versus those obtained using the refined model (Fig. 7) it is evident that the measurements in the DEM are about 20 cm above the base that marks the dry lake level. This might be explained by the fact that when the LiDAR data of the area were acquired, the deepest parts of the lake had some water, preventing the data acquisition or, alternatively, recording the elevation of the water surface.

7. Conclusions

The method constitutes a novel approach for characterizing the water surface, elevation, and volume of inland water bodies. It is based on freely-available satellite images provided by ESA and USGS, and in the availability of a sufficiently accurate DEM model of the lakebed.

The application of techniques capable of extracting SDSs with sub-pixel accuracy together with the refinement for deducting the mean elevation of the water level allow obtaining a robust and continuous estimation of the water stored in the Gallocanta Lake between 1984 and 2020. The proposed solution is supported by the combined use of images from different satellites. It enriches the existent data based on ground-based water level measurements, which have poor robustness during low water levels of the lake and do not consider the water surface dimension. The large amount of data derived in this study allows the analysis of yearly and seasonal trends along decades, as well as the quantification of short-term water changes, even those of small magnitude. This enables to verify how the lake's hydrological system responds to rainfall events in its watershed, opening up a promising possibility for advancing our knowledge of the hydrological dynamics of semi-arid environments. In addition, it allows differentiating modal states from extraordinary states, either by filling or emptying, which may be associated with particular hydro-meteorological situations. Likewise, the data show the existence of a seasonal behavior, although with an irregular (non-systematic) character, as previously pointed out by other authors.

This method may be exported to other water bodies (lagoons, reservoirs, etc.) with intermittent behavior in order to support monitoring purposes as it is able to offer datasets covering large periods (both historical and present/future) with a large degree of automation. A future improvement could come from analyzing the correspondence between the modal altitudes predicted by the model and the active littoral forms recognizable on the shores, which appear distributed at different heights defining different degrees of frequency of inundation/activation.

CRediT authors statement

Author statement outlining the individual contributions to the paper, **J.Palomar-Vázquez**: Conceptualization, Methodology, Data curation, Software, Formal analysis, review & editing, **C.Cabezas-Rabadán**: Conceptualization, Methodology, Data curation, Visualization, Writing - original draft, review & editing, **C.Castañeda**: Conceptualization, Funding acquisition, review & editing, **F.J. Gracia**: Conceptualization, Funding acquisition, review & editing, **A. Fernández-Sarría**: Data curation, review & editing, **E.Priego-de-los-Santos**: Data curation, Resources, **R. Pons-Crespo**: Data curation, Resources, **J.E. Pardo-Pascual**: Conceptualization, Funding acquisition, Methodology, review & editing, Supervision, Project administration.

Supporting data

The complete shoreline contour, water level elevation and volumetric dataset for the Gallocanta Lake is publicly available at https://doi.org/10.1016/j.dib.2022.108437 (Palomar-Vázquez et al., 2022).

Declaration of competing interest

The authors declare that they have no known competing financial interests or personal relationships that could have appeared to influence the work reported in this paper.

Acknowledgments

References

Birkett, C. M. (1995). The contribution of TOPEX/POSEIDON to the global monitoring of climatically sensitive lakes. *Journal of Geophysical Research, 100.* https://doi.org/10.1029/95JC02125, 179–25.

Busker, T., De Roo, A., Gelati, E., Schwatke, C., Adamovic, M., Bisselink, B., Pekel, J. F., & Cottam, A. (2019). Global lake and reservoir volume analysis using a surface water dataset and satellite altimetry. *Hydrology and Earth System Sciences, 23*(2), 669–690.

Cabezas-Rabadán, C., Pardo-Pascual, J. E., & Palomar-Vázquez, J. (2021). Characterizing the relationship between the sediment grain size and the shoreline variability defined from sentinel-2 derived shorelines. *Remote Sensing, 13*(14), 2829.

Cabezas-Rabadán, C., Pardo-Pascual, J. E., Palomar-Vázquez, J., & Fernández-Sarría, A. (2019). Characterizing beach changes using high-frequency Sentinel-2 derived shorelines on the Valencian coast (Spanish Mediterranean). *Science of the Total Environment, 691*, 216–231.

Cabezas-Rabadán, C., Pardo-Pascual, J. E., Palomar-Vázquez, J., Ferreira, Ó., & Costas, S. (2020). Satellite derived shorelines at an exposed meso-tidal beach. *Journal of Coastal Research, 95*(SI), 1027–1031.

Castañeda, C., Gracia, F. J., Conesa, J. A., & Latorre, B. (2020). Geomorphological control on habitat distribution in an intermittent shallow saline lake, Gallocanta Lake, NE Spain. *Science of the Total Environment, 276*, Article 138601. https://doi.org/10.1016/j.scitotenv.2020.138601

Castañeda, C., Gracia, F. J., Luna, E., & Rodríguez-Ochoa, R. (2015). Edaphic and geomorphic evidences of water level fluctuations in the Gallocanta Lake, NE Spain. *Geoderma, 239–240*, 265–279.

Castañeda, C., & Herrero, J. (2005). The water regime of the Monegros playa-lakes established from ground and satellite data. *Journal of Hydrology, 310*, 95–110. https://doi.org/10.1016/j.jhydrol.2004.12.007

CHE (The Ebro River-Basin Authority). (2003). *Establecimiento de las normas de explotación de la unidad hidrogeológica "Gallocanta" y la delimitación de los perímetros de protección de la laguna.* Zaragoza, Spain: Confederación Hidrográfica del Ebro (In Spanish, Unpublished).

Chen, B., Chen, L. F., Huang, B., Michishita, R., & Xu, B. (2018). Dynamicmonitoring of the poyang lakewetland by integrating Landsat and MODIS observations. *ISPRS Journal of Photogrammetry and Remote Sensing, 139*, 75–87. https://doi.org/10.1016/j.isprsjprs.2018.02.021

Comín, F. A., Julià, R., Comín, M. P., & Plana, F. (1990). Hydrogeochemistry of lake Gallocanta (Aragón, NE Spain). *Hydrobiologia, 197*, 51–66.

Cooley, S. W., Ryan, J. C., & Smith, L. C. (2021). Human alteration of global surface water storage variability. *Nature, 591*(7848), 78–81. https://doi.org/10.1038/s41586-021-03262-3

Crétaux, J.-F., Jelinski, W., Calmant, S., Kouraev, A., Vuglinski, V., Bergé-Nguyen, M., & Cazenave, A. (2011). SOLS: a Lake database to monitor in the near real time water level and storage variations from remote sensing data. *Advances in Space Research, 47*, 1497–1507. https://doi.org/10.1016/j.asr.2011.01.004

Feyisa, G. L., Meilby, H., Fensholt, R., & Proud, S. R. (2014). Automated water extraction index: A new technique for surface water mapping using Landsat imagery. *Remote Sensing of Environment, 140*, 23–35.

Frappart, F., Calmant, S., Cauhopé, M., Seyler, F., & Cazenave, A. (2006). Preliminary results of ENVISAT RA-2-derived water levels validation over the Amazon basin. *Remote Sensing of Environment, 100*, 252–264. https://doi.org/10.1016/j.rse.2005.10.027

Galván, R. (2011). Evolución histórica de la laguna de Gallocanta. Un análisis documental. *Xiloca, 39*, 69–98 (In Spanish).

García-Vera, M. A., & Martínez-Cob, A. (2004). *Evolución del Contenido de Humedad y de la Tasa de Evaporación en Humedales: Aplicación a la Laguna de Gallocanta. 2004.* -PH-14-I, Zaragoza, Spain (In Spanish) Available on: http://digital.csic.es/bitstream/10261/2976/1/InformeGallocanta2004-DEF.pdf.

García-Vera, M. A., San Román, J., Blasco, O., & Coloma, P. (2009). *Hidrogeología de la Laguna de Gallocanta e implicaciones ambientales. En La Laguna de Gallocanta Medio Natural, Conservación y Teledetección.* Madrid: Memorias de la Real Sociedad Española de Historia Natural (In Spanish).

Gracia, F. J., Gutiérrez, F., & Gutiérrez, M. (2002). Origin and evolution of the Gallocanta polje (iberian range, NE Spain). *Zeitschrift für Geomorphologie N.F., 46*, 245–262.

Gstaiger, V., Huth, J., Gebhardt, S., Wehrmann, T., & Kuenzer, C. (2012). Multi-sensoral and automated derivation of inundated areas using TerraSAR-X and ENVISATASAR data. *International Journal of Remote Sensing, 33*(22), 7291–7304. https://doi.org/10.1080/01431161.2012.700421

Gulácsi, A., & Kovács, F. (2020). Sentinel-1-Imagery-Based high-resolution water cover detection on wetlands, aided by google Earth engine. *Remote Sensing, 12*, 1614.

Huang, C., Nguyen, B. D., Zhang, S., Cao, S., & Wagner, W. (2017). A comparison of terrain indices toward their ability in assisting surface water mapping from Sentinel-1 data. *ISPRS International Journal of Geo-Information, 6*(5), 140.

Li, J., & Chen, B. (2020). Global revisit interval analysis of landsat-8-9 and sentinel-2A-2B data for terrestrial monitoring. *Sensors, 20*(22), 6631.

Li, J., & Roy, D. P. (2017). A global analysis of Sentinel-2a, Sentinel-2b and Landsat 8 data revisit intervals and implications for terrestrial monitoring. *Remote Sensing, 9*, 902. https://doi.org/10.3390/rs9090902

Luna, E., Latorre, B., & Castañeda, C. (2014). *Rainfall and the presence of water in Gallocanta Lake. Proceedings of the IX European wetland congress, wetlands biodiversity and services.* Huesca, Spain: Tools for Socio-Ecological Development.

Martínez-Cob, A., Zapata, N., & Sánchez, I. (2010). *Viento y riego. La variabilidad del viento en Aragón y su influencia en el riego por aspersión.* Zaragoza, Spain: Institución Fernando El Católico.

Palmer, S. C., Kutser, T., & Hunter, P. D. (2015). Remote sensing of inland waters: Challenges, progress and future directions. *Remote Sensing of Environment, 157*, 1–8.

Palomar-Vázquez, J., Pardo-Pascual, J.E., Cabezas-Rabadán, C., Alonso-Aransay, D. Monitorizando los cambios de superficie y volumen de la Laguna de Gallocanta mediante imágenes Landsat-8 y Sentinel-2. X Jornadas de Geomorfología Litoral, 4-6 Sep., Castelldefels (In Spanish).

Palomar-Vázquez, J, Cabezas-Rabadán, C, Fernández-Sarría, A, Priego-de-Los-Santos, E, Pons-Crespo, R, Pardo-Pascual, J, Eliseu, et al. (2022). Shoreline contour, water level elevation and volumetric dataset (1984-2020) for the Gallocanta Lake (NE Spain). *Data in Brief, 43*(August 22), Article 108437. https://doi.org/10.1016/j.dib.2022.108437

Pardo-Pascual, J. E., Almonacid-Caballer, J., Ruiz, L. A., & Palomar-Vázquez, J. (2012). Automatic extraction of shorelines from Landsat TM and ETM+ multi-temporal images with subpixel precision. *Remote Sensing of Environment, 123*, 1–11.

Pardo-Pascual, J. E., Sánchez-García, E., Almonacid-Caballer, J., Palomar-Vázquez, J. M., Priego De Los Santos, E., Fernández-Sarría, A., & Balaguer-Beser, Á. (2018). Assessing the accuracy of automatically extracted shorelines on microtidal beaches from Landsat 7, Landsat 8 and Sentinel-2 imagery. *Remote Sensing, 10*(2), 326.

Pekel, J. F., Cottam, A., Gorelick, N., & Belward, A. S. (2016). High-resolution mapping of global surface water and its long-term changes. *Nature, 540*(7633), 418–422.

Penton, D. J., & Overton, I. C. (2007). Spatial modelling of floodplain inundation combining satellite imagery and elevation models. In *MODSIM 2007 international congress on modelling and simulation.* Clayton south, Vic, Australia: Modelling and Simulation Society of Australia and New Zealand CSIRO.

San Román, J., García, M. A., Blasco, O., & Coloma, P. (2007). Hidrogeología de la laguna de Gallocanta. *Xiloca, 35*, 65–86 (In Spanish).

Sánchez-García, E., Briceño, I., Palomar-Vázquez, J., Pardo-Pascual, J., Cabezas-Rabadán, C., & Balaguer-Beser, Á. (2019). Beach Monitoring Project on Central Chile. In *5ª Conferència sobre Morfodinàmica Estuarina e Costeira, MEC2019, 20-24 Jun., Lisboa.* ISSN: 978-989-20-9612-4.

Sánchez-García, E., Palomar-Vázquez, J. M., Pardo-Pascual, J. E., Almonacid-Caballer, J., Cabezas-Rabadán, C., & Gómez-Pujol, L. (2020). An efficient protocol for accurate and massive shoreline definition from mid-resolution satellite imagery. *Coastal Engineering, 160*, Article 103732.

Schwatke, C., Dettmering, D., Börgens, E., & Bosch, W. (2015). Potential of SARAL/AltiKa for inland water applications. *Marine Geodesy, 38*, 626–643. https://doi.org/10.1080/01490419.2015.1008710, 2015b.

Timms, B. V. (1992). *Lake geomorphology.* Adelaide: Gleneagles Publishing.

Villadsen, H., Andersen, O. B., Stenseng, L., Nielsen, K., & Knudsen, P. (2015). CryoSat-2 altimetry for river level monitoring – evaluation in the Ganges-Brahmaputra River basin. *Remote Sensing of Environment, 168*, 80–89. https://doi.org/10.1016/j.rse.2015.05.025, 2015.

Xing, L., Tang, X., Wang, H., Fan, W., & Wang, G. (2018). Monitoring monthly surface water dynamics of Dongting Lake using Sentinel-1 data at 10 m. *PeerJ, 2018*(6), Article e4992. PeerJ Inc. Retrieved April 19, 2021, from http://www.ramsar.org/wetland/china.

Zhang, G., Chen, W., & Xie, H. (2019). Tibetan Plateau's lake level and volume changes from NASA's ICESat/ICESat-2 and Landsat Missions. *Geophysical Research Letters, 46*(22), 13107–13118. https://doi.org/10.1029/2019GL085032

Zhang, G., Xie, H., Kang, S., Donghui, Y., & Ackey, S. (2011). Monitoring lake level changes on the Tibetan Plateau using ICESat altimetry data (2003-2009). *Remote Sensing of Environment, 115*, 1733–1742. https://doi.org/10.1016/j.rse.2011.03.005

Zheng, J., Ke, C., Shao, Z., & Li, F. (2016). Monitoring changes in the water volume of Hulun Lake by integrating satellite altimetry data and Landsat images between 1992 and 2010. *Journal of Applied Remote Sensing, 10*(1), Article 016029.

Zhou, Y., Dong, J., Xiao, X., Liu, R., Zou, Z., Zhao, G., & Ge, Q. (2019). Continuous monitoring of lake dynamics on theMongolian Plateau using all available Landsat imagery and Google Earth Engine. *Science of Total Enviornment, 578*, 366–380. https://doi.org/10.1016/j.scitotenv.2019.06.341

Zhu, W., Jia, S., & Lv, A. (2014). Monitoring the fluctuation of lake Qinghai using multi-source remote sensing data. *Remote Sensing, 6*, 10457–10482.